

M. Parlier, M.-H. Ritti, A. Jankowiak  
(Onera)

E-mail: michel.parlier@onera.fr

# Potential and Perspectives for Oxide/Oxide Composites

The challenge for oxide/oxide composites is to provide an alternative to SiC/SiC composites with the aim of decreasing the cost of manufacture and improving the thermal stability in air at high temperature. Oxide/oxide composites consist of a porous alumina matrix reinforced by fibers of the same nature. Obtaining a controlled rate of porosity in the preparation helps to dissipate the energy associated with the propagation of cracks in the matrix during loading. It follows that the composite is damage-tolerant without requiring a carbon coating on the fibers as in the case of SiC/SiC composites. Using submicron alumina powders and specific additives necessary for shaping and for control of the sintering shrinkage, the first composites were obtained by developing a method of infiltration into fibrous reinforcements. To increase the fiber volume fraction and thus the mechanical properties, processes based on the prepreg molding in a plastic bag of a suspension in a fiber preform were selected. The development of these various processing routes is outlined in relation with the evolution of properties. The development of thermal barrier coatings based on microporous oxide is also presented, in order to extend the thermostructural potential beyond 1200°C.

## Introduction

Over the last decades, considerable efforts have been devoted to the improvement of the temperature capability of metallic superalloys, which cannot henceforth exceed 1150°C. For structural applications at higher temperatures under high stresses in oxidizing and corrosive environments, ceramic materials are promising candidates, provided that their brittleness can be overcome by using continuous fiber reinforcements. Since the research performed in the early 80's with the first generation of ceramic fibers, Ceramic Matrix Composites (CMCs) have shown their ability to exhibit a damage-tolerant behavior (Box 1).

Nevertheless, while CMCs have experienced an exceptional development over the last decade, mainly in the short term in the field of aerospace applications (missiles, rocket propulsion) where there is a constant need to increase payloads and working temperatures, efforts are now focused on cost reduction and on the improvement of the life duration. The objective is to use these new materials in gas turbine engines to improve their efficiency and to reduce polluting emissions [1].

Beyond the concept of weak interface composites (WICs) and to overcome the oxidation of the interphase between the fiber and the matrix (see box 1), the challenge was to develop a non oxidizable composite. The first step was to establish the feasibility and the potential of

an oxide/oxide composite for a hot combustor wall. A single crystal alumina fiber (Saphikon, USA)/zirconia ( $ZrO_2$ ) interphase/alumina matrix has been developed and tested in the frame of the NOXICC Brite/Euram program (Novel OXide Ceramic Composites) [2]. After ageing at 1400°C for 100 and 1000 hours, it has been shown that the mechanical behavior remains comparable to the as-processed composites [3].

To decrease the cost, the next step described in this paper was to develop a weak matrix concept without interphase, using Nextel fibers produced by the 3M Company (USA) to reinforce a porous alumina matrix. The technique to produce the porous alumina matrix, i.e. infiltration of powder followed by sintering, is described in § «Elaboration by infiltration». The mechanical performance and the procedure of improvement of the 2D Nextel 720/ $Al_2O_3$  composite are then discussed in § «Mechanical behavior» and § «Improvement of mechanical properties, respectively». A potential application concerning hot wall combustor chambers, various thermal barrier coatings (TBCs) are investigated in § «Evaluation of thermal barrier coatings» to increase the working temperature of the composite in hot gas up to 1500°C. Simulation of thermal barrier thickness and ageing behavior are also reported. Finally, to improve the fiber volume fraction and thus the mechanical properties, the first results on 2D Nextel 610/ $Al_2O_3$  composites produced by prepreg molding in plastic bags are presented.

## Box 1 - Damage-tolerant behavior of CMCs

The advent of high temperature components manufactured in CMCs originates from the ability of this class of materials to exhibit a dissipative damage-tolerant behavior, as opposed to monolithic ceramics, which exhibit brittle fracture induced by crack initiation and propagation from the statistical flaw distributions (figure B01-1). This particular property of CMCs is characterized by the development of matrix multicroacking without fiber breaking, a rather unexpected behavior for a material made of two brittle constituents. It is the result of achieving during processing a fiber-matrix bonding sufficiently weak to allow debonding and consequently the relaxation of the stress field at the crack tip and the bridging of matrix cracks by the fibers.

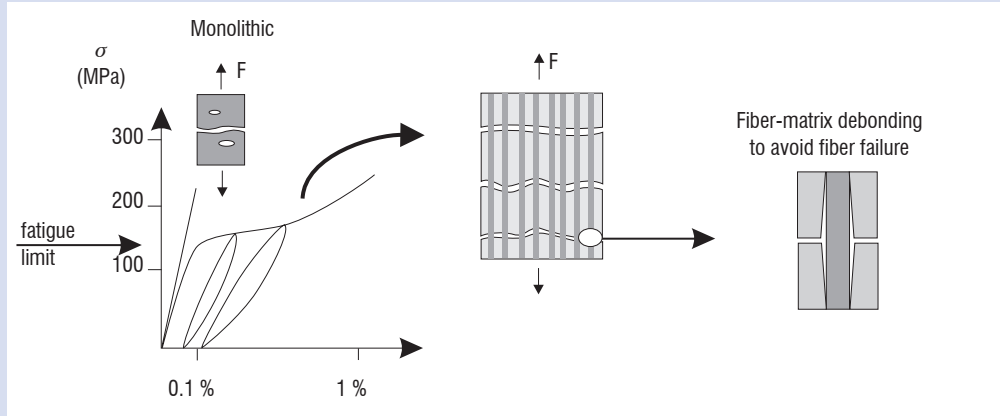


Figure B01-1 – Damage tolerant behavior of CMCs compared to monolithic ceramic

From the well known relationship presented by He and Hutchinson [4], the fracture energy of the interface ( $\Gamma_I$ ) for this debonding initiation process can be calculated in relation to the fracture energy of the fiber ( $\Gamma_F$ ). A ratio  $\Gamma_I/\Gamma_F \leq 0.25$  must be respected to achieve a non brittle behavior when the fiber and the matrix exhibit similar Young's moduli,  $E_F$  and  $E_M$ , respectively (figure B01-2). For CMCs with dense and crystalline matrices (e.g. SiC,  $Al_2O_3$ ) surrounding the fiber, the deposition on the fiber of a thin coating called interphase with low cohesion (e.g. pyrolytic carbon or boron nitride, etc.) is required for lowering  $\Gamma_I$ . CMCs of this type are called Weak Interface Composites (WICs). Nevertheless, these coatings may be oxidized at high temperature, thus leading to an increase in the relative fracture energy  $\Gamma_I/\Gamma_F$  and consequently to a brittle failure of the WIC. In the case of Weak Matrix Composites (WMCs) characterized by a matrix with a fine porosity, the reduced matrix stiffness ( $E_M < E_F$ ) and strength allow a damage-tolerant behavior, even in the case of a strong matrix-fiber interface. Nevertheless, since the matrix is not able to sustain a significant load, the mechanical behavior of WMCs is dominated by the properties of the fibers and a low strength is obtained under compression. Furthermore, brittle failure can be observed if the matrix is excessively densified during the manufacturing step (e.g. infiltration of precursors, sintering of powders, etc.).

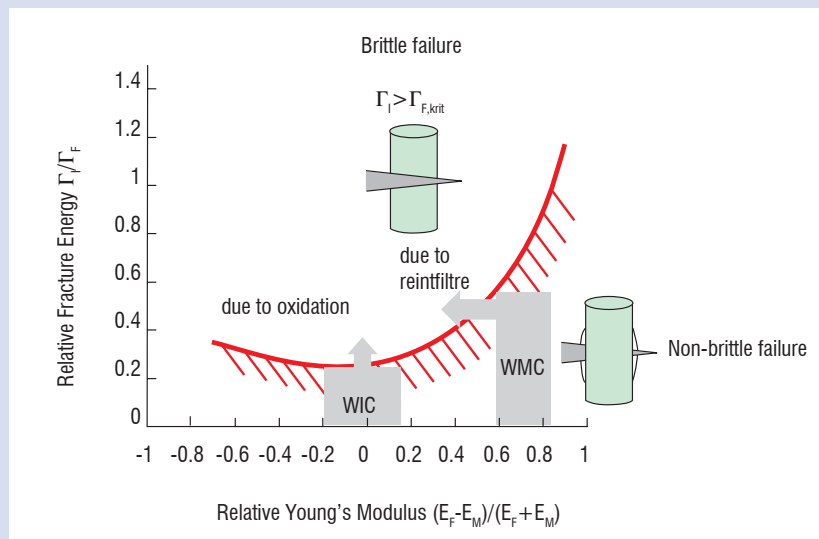


Figure B01- 2 – Boundary curve for non brittle failure of CMCs, taking into account the relative fracture energy  $\Gamma_I/\Gamma_F$  and the relative stiffness of fiber and matrix [4]. Additionally, the effect of interfacial oxidation and matrix densification are illustrated [5].

## Elaboration by infiltration

One way to produce an oxide matrix is to use a Sol-Gel process, where liquid alkoxide precursors are infiltrated into the fiber preform to form a polymeric oxide network (gel) in situ, via hydrolysis and polycondensation reactions. Nevertheless, the first step of the gel formation and its subsequent pyrolysis are globally characterized by a low mass yielding of ceramics, thus leading to a high level of shrinkage (~ 80%). To counterbalance this limitation, a two-step infiltration technique has been developed [5]. The first step consists in an infiltration of the fiber preform by fine submicronic oxide particles using a slurry filtration technique, which allows about 50% of the free volume to be filled. Then, the residual porosity of the powder infiltrated in the fiber preform is filled with an alkoxide followed by in situ hydrolysis/polycondensation and pyrolysis, leading to the formation of an efficient binder. For applications in rocket propulsion, the validity of this processing route has been shown on alumina infiltrated in carbon fiber preforms produced by Snecma (Novoltex®). In this case, a judicious combination of two alkoxides has been selected, firstly, to reduce the shrinkage of the matrix and, secondly, to increase the mechanical properties via the reduction of porosity [6].

The Nextel fibers used in this study are alumina based systems produced by 3M. Nextel 720 is a mixture of alumina and mullite ( $2\text{SiO}_2\text{-}3\text{Al}_2\text{O}_3$ ), developed to achieve a compromise between strength and creep with a proven thermal stability up to 1200°C. Nextel 610, mainly composed of alumina, was also used to reach a higher modulus, but its maximum working temperature is limited to 1100°C for long term applications. Since the objective was to moderately densify the matrix, in order to produce a weak matrix composite, the strategy adopted was to select an alumina powder able to sinter at a moderate temperature ( $\leq 1200^\circ\text{C}$ ), with limited shrinkage to avoid matrix multi-cracking. The introduction of Sol-Gel was investigated in a second step § «Improvement of mechanical properties» to check its potential to improve the mechanical performance after ageing.

### Sintering behavior of alumina powders

Initially, the objective was to compare the sintering behavior of several alumina powders characterized by a small particle size, to promote their infiltration into Nextel tissues: alpha alumina from the Baikowski Company (France), boehmites AIO (OH) from the Sasol Company (South Africa) (table 1).

Powder	Crystallization	d50 (d20-d90) $\mu\text{m}$	Specific surface area $\text{m}^2/\text{g}$	Size of dispersed particles $\mu\text{m}$	Green density
A1	Alpha	1.1 (0.7-2.5)	3		1.5
A2	Alpha	0.3 (0.2-0.7)	10		1.9
B1	Boehmite	45	260	0.025	1.2
B2	Boehmite	50	200	0.090	1.5
B3	Boehmite	40	100	0.220	1.4

Table 1- Characteristics of alumina and boehmite powders

The comparison of the sintering shrinkage on pressed pellets (uniaxial press, 60 MPa) is shown in figure 1 as a function of temperature (heating rate of 300°C/h). Both alpha alumina are not sintered very much at 1200°C. However, the A2 powder is characterized by a slightly higher shrinkage, due to its finer particle size. On the other hand, the shrinkage is much more important with boehmites. This behavior is related, firstly, to the loss of hydroxyl groups at low temperatures and, secondly, to the finer individual particle size.

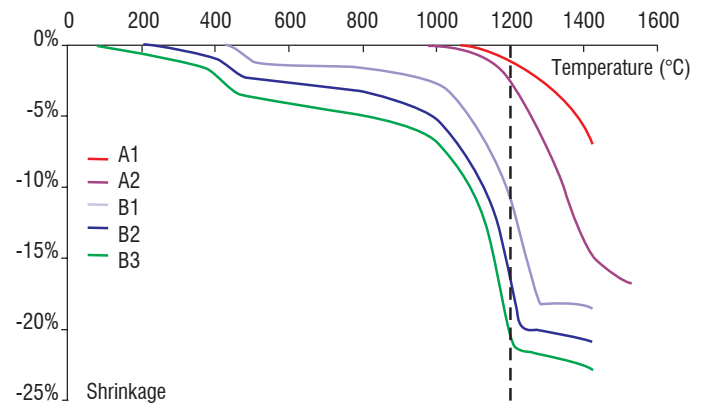


Figure 1 - Evolution of linear sintering shrinkage of alumina powders (300°C/h)

Since the thermostability of Nextel 720 fibers does not exceed 1200°C, the sintering of the composite was deliberately limited to this temperature. Moreover, the presence of the fiber reinforcement (weaving in both directions of the plane) prevents the volume shrinkage of the matrix, thus leading to a severe cracking of the latter. Therefore, only the powders with the lowest shrinkage at 1200°C have been retained in the remainder of the study: alpha alumina A2 and A1, boehmite B3.

### Rheology of alumina suspensions

Whatever the processing technique, trials have shown that it is preferable to minimize the amount of water to reduce the level of porosity. However, the rheology of suspensions should be adjusted to get a good infiltration of the powder within the heart of the strands.

To optimize the suspension of A2 alumina powder, viscosity was measured according to the mass concentration of the powder (mass of powder/water) and pH (figure 2). For this, various suspensions in water were prepared, with different additions of concentrated nitric acid or alumina powder to modify the pH and mass concentration, respectively. A viscosimeter with coaxial cylinders (Rheologic International RI:2:L) was used to measure the viscosity, following the DIN 53019 procedure with cylindrical geometry (spindle and sample chamber with a diameter of 14 mm and 15 mm respectively) and shear rate of 10  $\text{s}^{-1}$ .

The concentration of 1335 g/l corresponds to the suspension used during the vacuum-pressure infiltration. Its viscosity is very low (4.7 mPa.s). When doubling the concentration by simply adding powder, the pH then increases from 4.7 to 5.6 and the viscosity rises by ten, but the variation is small for pH between 5.6 and 3.9.

Until the concentration of 4000 g/l is attained, the viscosity remains low (60 mPa.s). On the other hand, the viscosity is multiplied by a factor of 4 for an additional increase of 10% in the concentration (210 mPa.s for 4320 g/l).

	Woven fabric	Number of plies	Matrix	Fiber vol. fraction $V_f$ (%)	Density	Porosity (%)	Comment
1	Nextel 440	3	A1	17	1.84	49	Low Vf
2		14		31	1.5	53	Low infiltration yield
3		3	B3	18	1.57	53	Low Vf
4		9		35	1.70	47	High porosity
5	Nextel 720	7	A2	28	2.78	23	Satisfactory densification
6		7		32	2.82	24	
7		8		37	2.81	23	
8		8		37	2.81	23	

Table 2 - Synthesis of infiltration in Nextel fabrics

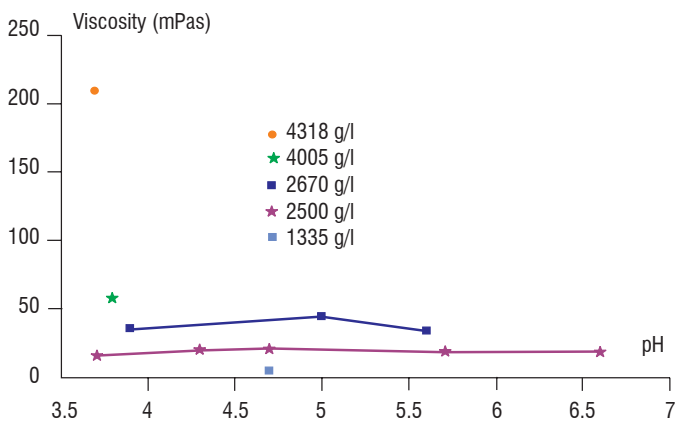


Figure 2 – Change in the viscosity of alumina suspensions versus pH for various concentrations

The viscosity level is not in itself the only criterion to be considered. Indeed, we must also consider the shear stress required to displace the suspension. According to measurements, the shear stress can change very quickly (500 to 3700 mPa) depending on the pH, so that the viscosity is not affected. Moreover, during acidification of suspensions by concentrated nitric acid, hard powder agglomerates are locally formed and they are difficult to re-disperse. This is especially true with a low pH ( $< 4$ ) and a high concentration.

Thus, the use of concentrated suspensions is possible, but difficult to master as a function of pH, or at least on the way to introduce the acid. These measurements have also shown that prepreg infiltration could certainly be improved by optimizing the concentration and pH.

### Infiltration of fabrics

Nextel 720 fabric was supplied by 3M France for the purposes of this study. It is a satin weave of 8 (Ref 720 Nextel XN-513 - Wireless 1500 denier). A similar tissue in Nextel 440 has also been used for a preliminary development.

To infiltrate the layers of fabrics by powders, they are placed on a filter and the thickness of the stack is fixed by a top gate, in order to control the fiber volume fraction. The suspensions consist of water with  $\text{pH} = 3$  (addition of nitric acid) and powder in equal proportions

by mass to reach about 2600g/l. To facilitate the migration of the powder suspension within the fabrics, a vacuum under the filter and pressure (0.2 MPa) in the upper assembly are required. The water of the suspension is thus evacuated in the lower part, while the powder is infiltrated between the fibers. After drying, the materials are sintered at 1200°C for one hour.

The results of the infiltration into Nextel 440 and 720 tissue stacks are shown in table 2. The first tests were conducted on the Nextel 440 for economy. For the A1 powder, there is an inadequate infiltration (composites 1 and 2), even with a limited number of plies, which results in a high porosity. For the B3 powder, the lowest particle size is preferable to achieve a better infiltration. Moreover, the decomposition of boehmite (loss of OH radicals) leads naturally to a higher shrinkage and therefore to matrix microcracking induced by the presence of fibers hampering shrinkage (composites 3 and 4). Consequently, the porosity is too high.

On the other hand, the A2 powder, characterized by a low shrinkage and an intermediate particle size, leads to a good infiltration rate and a much lower porosity (composite 5). This result was confirmed with Nextel 720 fabrics (composites 6, 7 and 8). Globally, 2D Nextel 720/A2 composites (66 x 40 x 2.4 mm) are characterized by a fiber volume fraction of about 35% and a porosity of 23%.

## Mechanical behavior

### Flexural strength up to 1150°C

For 2D Nextel 720/A2 composites consisting of a stacking of 8 or 10 plies with mirror symmetry, some flexural tests (3 point configuration, specimen size: 66 x 7x 2.4 mm, support span: 30 mm, displacement rate : 0.3mm/mn) were performed at room temperature on specimens from different plates. The results of the three-point bending tests are reported in table 3 and table 4.

For three composites (7, 8, 9) with similar morphological characteristics (fiber volume fraction and porosity), a good uniformity of failure stress with an average value of 165 MPa can be noticed, a Young's modulus of 35 GPa and a damage tolerant behavior. A test was also performed on a composite having a higher fiber volume fraction (composite 10). This latter was obtained by adding two

layers of fabric to maintain the mirror symmetry, whereas the same thickness is imposed by the upper grid of the infiltration device. Paradoxically, one specimen exhibits the highest strength, while the other two are among the lowest recorded strengths. A rougher surface and a tendency to delamination of the outer plies can explain these poorer results. A slight relaxation of the more compressed plies is not excluded in this case, but the thickness measurements after sintering are not precise enough to confirm it.

High temperature tests were performed on composites with a stacking of 8 plies of Nextel 720 fabrics (composites 7 and 8). The results reported in table 4 highlight the significant increase in flexural strength with temperature (+ 45% at 1150°C).

	Porosity (%)	$V_f$ (%)	$\sigma_f$ (MPa)	$E_f$ (GPa)
7	23	37 8 plies	178	36
			145	29
8	23	37 8 plies	182	40
			153	33
9	23	35 8 plies	171	39
			164	36
			157	34
Average			<b>165</b>	<b>35</b>
10	22	43 10 plies	125	32
			184	48
			125	25
Average			<b>145</b>	<b>35</b>

Table 3 – Morphological and mechanical characteristics of 2D Nextel 720/Al<sub>2</sub>O<sub>3</sub> composites

Temperature (°C)	$\sigma_f$ (MPa)	$E_f$ (GPa)
20	178	36
	145	29
	182	40
	153	33
Average	<b>164</b>	<b>34</b>
10000	212	30
	193	27
Average	<b>200</b>	<b>28</b>
1150	224	17
	228	23
Average	<b>225</b>	<b>20</b>

Table 4 – Mechanical properties of 2D Nextel/720 composites as a function of temperature

### Flexural strength after ageing

The flexural strength after thermal ageing in air (10 and 100 hours at 1100 and 1200°C) was also determined (composite 9) at room temperature (figure 3). After 100 hours of ageing at 1100°C, the reduction in strength is about 15%, whereas after ageing at 1200°C, it attains 20% after 10 hours of ageing and is slightly above 30% after 100 hours of ageing.

## Improvement of mechanical properties

Since the alumina matrix is not fully densified in the composites, further sintering may occur, depending on the conditions of temperature and duration in service. The unavoidable consequence of shrinkage associated with matrix sintering is a decrease in the mechanical properties of the composites, mainly due to degradation of load transfer between fibers and matrix (matrix microcracking, debonding between fiber and matrix). To limit these phenomena, the ATK COI Ceramics company (USA) has adopted the option of introducing colloidal alumina [6], but there is no information available concerning the process. Based on previous work conducted on C/Al<sub>2</sub>O<sub>3</sub> composites, addition of zirconia has been taken into account to decrease the risk of sintering in service [7]. The principle is based on the fact that zirconia is more refractory than alumina (melting at 2690 and 2050°C, respectively) which results in a lower sintering (optimum densification at about 70% of the melting temperature).

The zirconia is introduced by infiltration of a zirconium alkoxide precursor in the porosity of the matrix partially consolidated by sintering. After hydrolysis/polycondensation and sintering, the precursor forms submicron zirconia grains arranged on the surface of the alumina grains and on the necks between the sintered grains. Moreover, the effect of silica was also tested on composites to confirm its role in the degradation of the mechanical properties after ageing. The silica is introduced by infiltration of a silicon alkoxide precursor.

### Precursor infiltration procedure

The production of composites is divided into several stages. Initially, we proceed to the infiltration of Nextel 720 fabric plies by the alumina powder. The composite obtained after drying is then sintered at 950°C to consolidate the powder, while maintaining the maximum porosity and promoting a damage-tolerant behavior. This step is essential to avoid matrix disintegration during the subsequent infiltration of the porosity by the liquid precursor. The main steps of injection and hydrolysis procedures of alkoxides are the following:

- drying at 120°C of the pre-sintered composite (950°C – 30 min);
- degassing of the hot composite in a dynamic vacuum (~ 2 hours);
- degassing of the alkoxide in a dynamic vacuum;
- introduction of the composite in alkoxide and complementary degassing for one hour in a static vacuum before returning to atmospheric pressure;
- hydrolysis of the composite over a steam bath for one hour;
- drying at 120 °C;
- sintering at 1200 °C for one hour.

Four composites were impregnated with a solution of 70 wt% of zirconium propoxide in propanol (Fluka 96595). Since this solution exhibits a high viscosity, partial infiltration was suspected, particularly in view of the dispersion in the results of the mechanical tests. Two other plates were therefore injected with a diluted solution of 54.5 wt% of zirconium propoxide in propanol. The mass uptake of composites has been difficult to estimate, because there is always a surplus at the surface (between 1 and 2.5 wt%). A plate of Nextel 720/Al<sub>2</sub>O<sub>3</sub> composite was impregnated with tetraethoxysilane (TEOS) as a precursor of silica. The porosity of 28% before injection was reduced to 24% after sintering.

## Results

After sintering, five specimens were cut in each plate, in order to perform three point bending tests. Two tests were used as a reference and the other three specimens were aged at 1200°C for 10 or 100 hours. The mean flexural strengths are reported in figure 3.

The composite infiltrated with the concentrated precursor is very promising, because the mechanical properties are slightly improved at room temperature and this level is maintained after ageing for 10 hours at 1200°C. However, the dispersion in strength is large, about 100 Mpa, due to the inhomogeneous distribution of zirconia. A more homogenous infiltration is achieved with the diluted precursor, which leads to a higher strength and a smaller dispersion.

The composites reinfiltred with a silica precursor exhibit a lower strength (115 MPa) and a 30% drop in strength after ten hours of ageing at 1200°C.

In conclusion, this early work on the reinfiltred of composites with precursors highlights the advantage of zirconia to improve, not only the reference mechanical properties, but also those measured at room temperature after thermal ageing. A similar approach was adopted by the Zok team at the University of California. The mechanical properties of composites are then improved by decreasing the porosity with an alumina precursor [8].

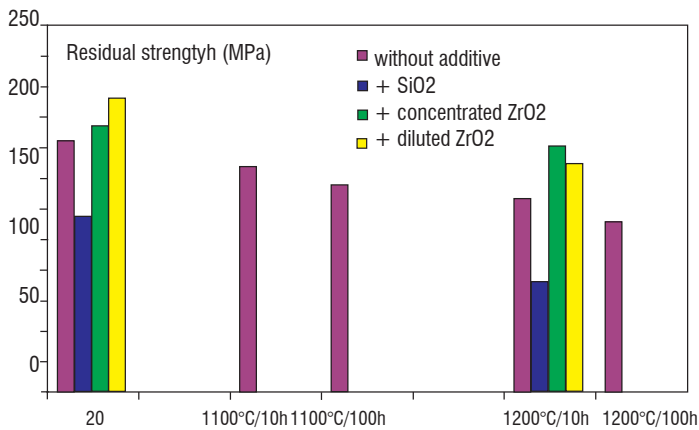


Figure 3 – Average residual flexural strength ( $\pm 10\%$  dispersion) after ageing of 2D Nextel 720/  $\text{Al}_2\text{O}_3$  composites with and without additives

## Evaluation of thermal barrier coatings

For applications with very long durations ( $> 100$  hours), it is preferable to limit the temperature to 1100°C to avoid the strength drop of the Nextel 720 fiber. However, to increase the maximum temperature that can be withstood by the composite, a thermal barrier coating (TBC) can be added, as shown by Solar Turbines (USA) for combustion chambers [9]. Initially, the potential of various TBCs was investigated, via the determination of their thermal conductivity in relation with their morphological and structural evolution. Then, thermal simulations were performed to determine the most efficient TBC for a given thickness.

### Alumina and mullite TBCs

The two main criteria to be considered in the selection of a TBC material are the chemical compatibility and thermal expansion agreement

with the composite. As major constituents of the TBC, alumina and mullite were naturally selected. Moreover, thermal conductivity of TBCs being very dependent on the porosity and morphology, various ways of production were taken into consideration to investigate the effect of these factors [10].

The two techniques most commonly used for ceramic coatings are plasma spraying and dipping in a suspension followed by sintering. These techniques were therefore used to produce alumina and mullite coatings. For alumina coating, another possibility is to use a reaction–bonding process based on the oxidation of aluminum /alumina powder mixtures. As described in box 2, this technique leads to porous Reaction Bonded Aluminum Oxide (RBAO) with higher mechanical strength as compared to conventional sintering. Furthermore, a high porosity level can be achieved using a dipping technique to deposit the  $\text{Al}/\text{Al}_2\text{O}_3$  slurry previously to the reactive sintering. A similar procedure can be used to produce mullite by reactive sintering from a slurry of polydimethylsiloxane/ $\text{Al}/\text{Al}_2\text{O}_3$  [13]. The characteristics of TBCs and N720/ $\text{Al}_2\text{O}_3$  composite are reported in table 5.

	Porosity (%)	CTE ( $10^{-6}\text{C}^{-1}$ )	Young modulus (GPa)	Poisson ratio	Flexural strength (MPa)
N 720/ $\text{Al}_2\text{O}_3$	25	6.2	40	0.2	140
RBAO	70	8	34	0.27	10
Mullite	40	5	58	0.27	40

Table 5 – Thermo-mechanical data of TBCs and composite necessary for residual thermal stress calculations

The thermal conductivity  $K$  ( $\text{W}/\text{m}\cdot\text{C}$ ) of composites and coatings was determined from measurements of thermal diffusivity  $D$  ( $\text{m}^2/\text{s}$ ), using a laser flash method. From the knowledge of the density  $\rho$  ( $\text{kg}/\text{m}^3$ ) and of the variation of the specific heat  $C_p$  ( $\text{J}/\text{kg}\cdot\text{C}$ ) with temperature, thermal conductivity is obtained by applying the relation  $K = D \cdot \rho \cdot C_p$

Diffusivity measurements were performed on discs, 20mm in diameter, machined in monoliths. For coatings prepared by thermal spraying, the measurements were performed directly on the coated composites taking into account its own thermal diffusivity. The thermal conductivities of the various alumina and mullite are respectively illustrated in figure 4 and figure 5.

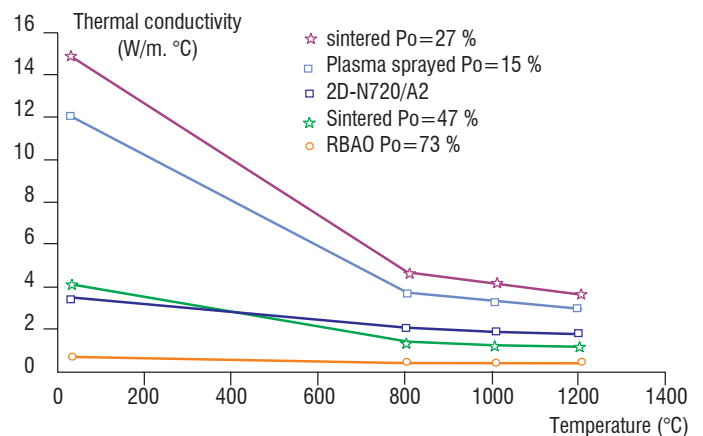


Figure 4 – Thermal conductivity of  $\text{Al}_2\text{O}_3$  TBC

The thermal conductivity decreases considerably with an increase in the porosity level, for the various sintered alumina. For the plasma-

## Box 2 - Reaction Bonded Aluminum Oxide (RBAO)

Another way to form an alumina matrix is the reaction-bonding process, based on the oxidation of aluminum/alumina powder mixtures [11]. The main advantage of this route is the possibility of producing almost net-shaped components, owing to the fact that the sintering volume shrinkage is counterbalanced by the expansion associated with the formation of alumina from aluminum. After investigating the oxidation mechanisms of aluminum powder and then of various Al/Al<sub>2</sub>O<sub>3</sub> mixtures, taking into account parameters such as the size of the powders, the thermal treatment and the mixture and pressing modes, it was possible to select a nuance (40/60% in volume) characterized by a close to zero shrinkage (Figure B2-01).

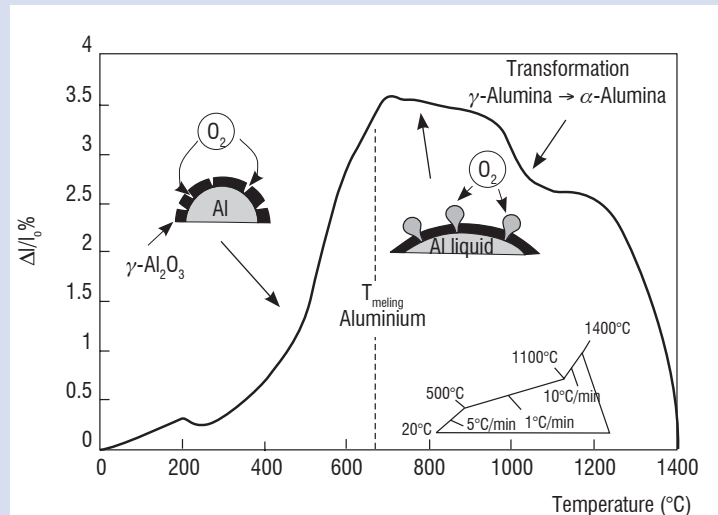


Figure B2-01 – Dimensional variations and oxidation mechanisms of the Al/Al<sub>2</sub>O<sub>3</sub> system during the reaction bonding of alumina

The addition of an activator, such as magnesia, improves the sintering kinetics and promotes a better densification at low temperature, despite the formation of vermicular alpha alumina, which is difficult to sinter below 1600°C. In addition, the presence of impurities such as iron leads to a better intergranular cohesion, which, with an equal porosity (34%), results in better mechanical properties (Figure B2-02): 270 MPa (sintering at 1250°C) instead of 175 MPa (sintering at 1400°C) for alumina with a residual porosity of 20% [12].

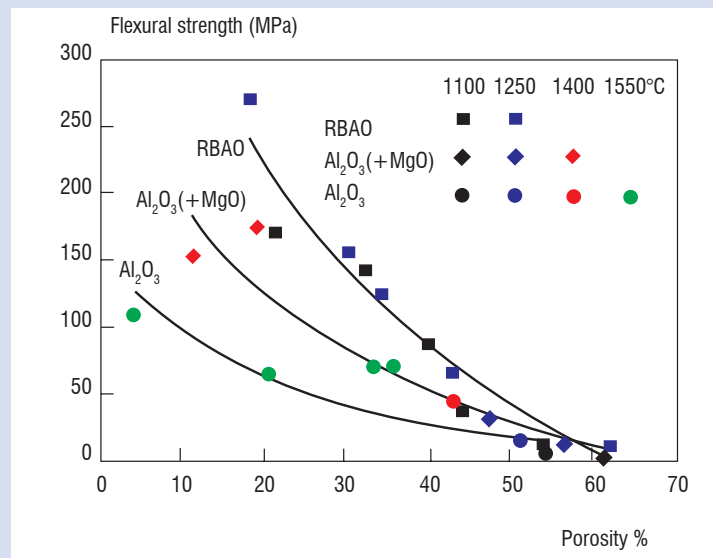


Figure B2-02 – Flexural strength versus porosity of different alumina monoliths conventionally sintered or processed

spayed alumina, the value determined for the composite is not representative, since the coating is completely debonded after the measurement of diffusivity up to 1200 °C. This behavior was correlated with a significant decrease in its porosity (25 to 12%), which is due to densification, as revealed by the morphological observations. The lowest thermal conductivity is obtained with the RBAO coating, which exhibits a very high level of porosity (75%).

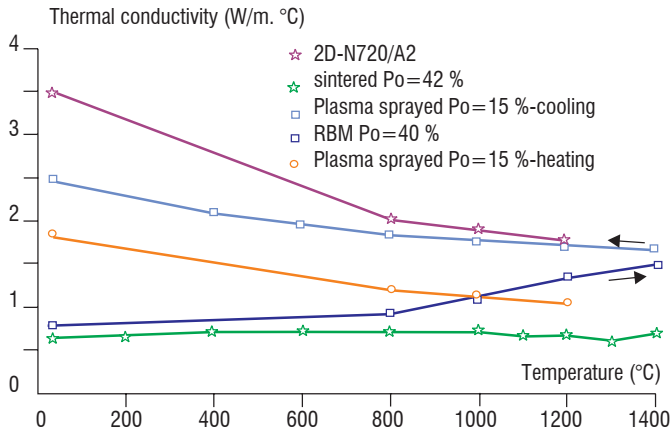


Figure 5 – Thermal conductivity of mullite TBC

For the plasma-spayed mullite, an increase in thermal conductivity is observed during the measurement. In this case, there is no significant reduction in porosity as in the case of thermal-spayed alumina, but there is a significant crystallization of mullite. Contrary to RBAO, the porosity of the reactive-bonded mullite (RBM) is lower (40%) and yttrium silicate has been added to improve the mechanical properties. Consequently, its thermal conductivity is higher than that of the RBAO coating. Finally, the lowest thermal conductivity is achieved with the mullite coating obtained by natural sintering of a submicron powder deposited by dip coating.

From the thermal conductivity measurements, we must bear in mind the very low thermal conductivity of RBAO (0.3 W/m°C) and of sintered mullite (0.7 W/m°C). In both cases, the thermal conductivity is stable, contrary to that of the thermal sprayed coatings, which evolves rapidly during use.

### Efficiency of TBC

From these conductivity values, a simulation of thermal barrier thickness was performed, using a thermal code developed at Onera [14]. The calculations reported in figure 6 were conducted in a combustion chamber configuration as follows:

- cylindrical combustion chamber made of 2D Nextel 720/ $Al_2O_3$  composite, with a TBC introduced in the inner part;
- combustion temperature of 1500 °C and exchange coefficient of 1000 resulting in a surface temperature of 1400°C for the TBC;
- external cooling of the composite by air at 600°C and with an exchange coefficient of 10 and an emissivity of 0.7 (common value for oxides at this temperature).

If the temperature at the interface between the TBC and the composite is fixed at 1100°C to avoid matrix ageing, only 1 mm of RBAO is necessary instead of 2.3 mm of sintered mullite. For the mullite obtained using reactive sintering, a thickness of 3.5 mm is required, owing to its higher thermal conductivity. Although it is compulsory to

increase the thickness of the thermal barrier when replacing alumina by mullite, the calculated thicknesses are lower than those used by Solar Turbines in their engine tests [9].

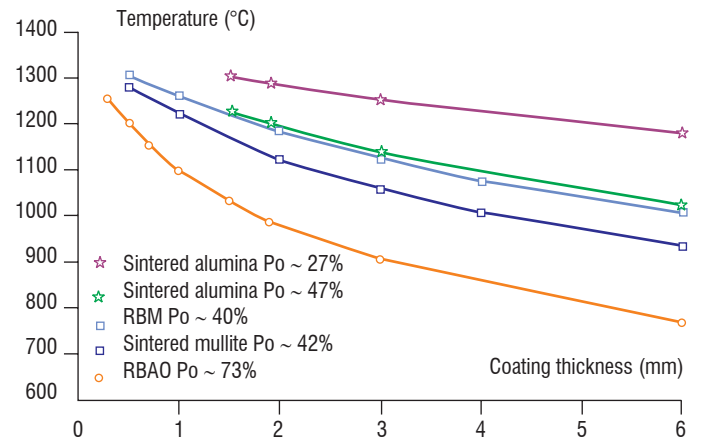


Figure 6 – Prediction of TBC thickness depending on the surface temperature of the composite

### Ageing behavior of TBCs

Since RBAO is the most efficient TBC according to thermal simulation, the latter has been selected first to evaluate the ageing behavior of different assemblies. RBAO plates were produced with a porosity level of 75% and a thickness of 1mm. Then, these plates were bonded to alumina monoliths or to 2D Nextel 720/alumina composites using two bonding suspensions: i) alumina A2 powder in water at pH=3, ii) mixture of alumina A2 and silica (mullite proportion) powders in water at pH=3.

In both cases, the suspension was deposited as a thin layer on monoliths or composites. Prior to this, they were soaked in water to prevent premature drying of the surface. As soon as the application of the suspension was completed, the RBAO TBC was deposited onto it and, finally, drying (in air and then in an oven) was performed by maintaining a constant pressure, using clamps to promote contact. Excess suspension was also removed during this operation.

All of the assemblies were sintered at 1200°C for 1 hour. They were then subjected to different thermal ageing treatments: 100 hours at 1100°C, then 100 hours at 1200°C. Following these treatments, we made sure there was no significant change in the microstructure of RBAO, as evidenced by the porosity measurements: 81% after sintering at 1200° C, 80.9% after 100h at 1100°C and 80.1% after 100h at 1200°C.

On monolithic alumina, the RBAO TBC is well joined with an alumina bonding layer after ageing, while a partial separation is observed with a mullite bonding layer. Breaking of the joining is observed in 2D Nextel 720/alumina composites, regardless of the nature of the binder. When the latter is made of alumina, the fracture occurs in this layer. On the other hand, for the mullite bonding, breaking occurs between this layer and the RBAO TBC.

To better identify the origin of the breakdown of RBAO TBC between alumina monolith or composite, their respective coefficient of thermal expansion (CTE) was measured (figure 7). The average CTE difference of about  $2.10^{-6}C^{-1}$  is largely sufficient to induce rupture, due to the development of residual thermal stresses during cooling. Never-



theless, for a mullite TBC, the CTE is lower than that of the composite and the difference is reduced to  $1.10 \cdot 10^{-6} \text{ } ^\circ\text{C}^{-1}$ . The use of a mullite TBC would be, a priori, a more viable candidate than an alumina TBC, especially since the composite would subject the TBC to compression during cooling.

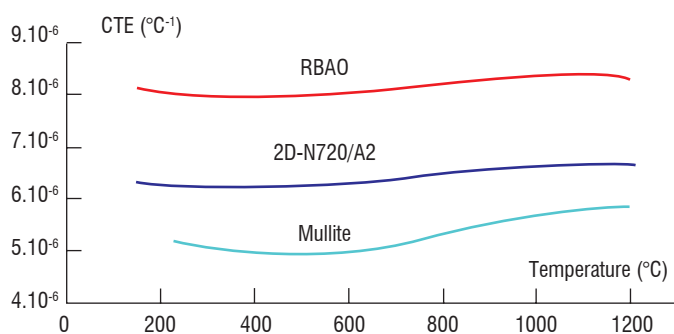


Figure 7 – Evolution of CTE with temperature for 2D Nextel 720  $\text{Al}_2\text{O}_3$  and for RBAO and mullite TBC

Consequently, a complementary ageing test was performed on a sintered mullite TBC with a porosity level of 40% and a thickness of 2 mm. This mullite TBC was joined to a 2D Nextel 720/alumina composite using the alumina bond. After ageing at  $1200^\circ\text{C}$  for 100 hours, no delamination of the assembly was noticed.

The analytical determination of the stress distribution was then performed in TBC and in composite to explain the behavior of the assembly submitted to ageing. Based on a Timoshenko analysis [15] adapted to a 2D asymmetrical system [16], calculations were performed using the thermo-mechanical data reported in table 5 and a  $\Delta T$  cooling range of  $1200^\circ\text{C}$ . It appears that the stress generated at the interface in RBAO, for the TBC/composite systems submitted to ageing (table 6), is higher than its flexural strength, thus leading to the initiation of cracks normal to the interface which, in turn, may promote debonding from the composite. On the contrary, for the mullite TBC, the rupture flexural strength is not attained on the free surface and the TBC layer near the interface is submitted to a compressive stress.

TBC on 2D N 720/ $\text{Al}_2\text{O}_3$	Stress in TBC (MPa)		Stress in composite (MPa)	
	surface	interface	interface	surface
1 mm RBAO / 2 mm composite	1	45	-58	35
2 mm mullite / 2 mm composite	34	-59	37	-15

Table 6 – Residual thermal stresses induced in TBC and in composite for the selected assemblies

## Perspectives for oxide/oxide

For a few years now, the elaboration processes generally used for organic matrix composites have been transposed to ceramic matrix composites such as vacuum-molding. Compared to infiltration techniques, these processes are cheaper and they allow the production of more complex shaped parts. Moreover, fiber volume fractions as high as 50% can be achieved. This last point is of great interest to improve

tensile strength and the Young's modulus, as explained in box 1 for Weak Matrix Composites [5], [18], [19], [21]. For all these reasons, new alumina/alumina composites were prepared using prepregs and vacuum molding procedures.

First, the alumina slurry previously used for the infiltration process is now used for impregnation of N610 fabrics (satin weave of 8, Ref 610 Nextel DF-11 - Wireless 1500 denier). Then,  $100 \times 150 \text{ mm}^2$  prepreg fabrics are stacked, vacuum bagged having standard bleeders and breathers and a low pressure is applied to reach a fiber volume fraction of 50%. Then, the temperature is raised up to  $100^\circ\text{C}$  to allow water evaporation from the composite. After drying, the as-processed plate is sintered at  $1200^\circ\text{C}$  with a short dwell time to limit fiber degradation. The final composite with a porosity of 25% exhibits excellent mechanical properties, with damage-tolerant behavior, as shown in table 7 and figure 8.

	Tensile tests	Flexural tests
$\sigma$ (MPa)	$275 \pm 15$	$229 \pm 74$
$\varepsilon$ (%)	$0.32 \pm 0.02$	-
E (GPa)	$140 \pm 6$	$122 \pm 21$

Table 7 – Summary of tensile and flexural properties for vacuum bagged N610/alumina composites

From figure 8, the tensile response is essentially linear with only small inelastic strain, as was usually observed in oxide-oxide composites [19], [20], [17]. Moreover, the mechanical behavior is quite reproducible. Compared to the N610/alumina composites made by Ruggles-Wrenn et al. [17], with an ultimate tensile strength of 117 MPa and a failure strain of 0.09%, the composites of this work are characterized by higher mechanical properties at room temperature.

Since the characteristics ( $V_f$ , density) of the two composites are similar, the great difference between the mechanical properties can be explained by the thermal treatment. Indeed, the sintering condition of the composites of Ruggles-Wrenn et al. is  $1200^\circ\text{C}$  for 5 hours. Such a long thermal treatment can induce fiber degradation and a decrease in the level of porosity of the matrix leading to a stiffer matrix, thus impeding the debonding process.

Papakonstantinou et al. [21] compared the mechanical properties of some CMCs. Hi-Nicalon (SiC)/SiC composites manufactured by chemical vapor infiltration (CVI) exhibit an ultimate tensile strength of 255 MPa, a Young's modulus of 230 GPa and a failure strain of 0.47%. The tensile strength of the N610/alumina composites produced by vacuum molding is close to that of the SiC/SiC composite, whereas the Young's modulus and failure strain are lower. The elastic moduli of the N610 fiber and the Hi-Nicalon fiber are respectively 373 GPa and 270 GPa [21]. As a consequence, the low Young's modulus of oxide/oxide composites (i.e., a 60% loss compared to fibers) is attributed to the weak matrix. For SiC/SiC composites, the decrease in the Young's modulus between the fibers and the composite is not so large ( $\sim 15\%$ ). This behavior can be explained by the nature of the fiber matrix interface. Indeed, SiC/SiC composites are considered as Weak Interface Composites (box 1) and so, the matrix is stiff but a fiber coating is necessary to allow a debonding mechanism, whereas it is not necessary for Weak Matrix

Composites. This comparison highlights the interest for oxide/oxide composites which are cheaper and less time consuming to manufacture, compared to SiC/SiC composites.

The mechanical properties of oxide/oxide composites can be adjusted, depending on the mechanical constraints required for applications such as exhaust parts or combustion chambers. As an example, to improve failure strain and creep behavior, some authors have coated the N610 fibers with monazite ( $\text{LaPO}_3$ ) [17]. As a result, strain is three times higher, tensile strength is increased but the elastic modulus is decreased and the manufacturing process becomes more expensive.

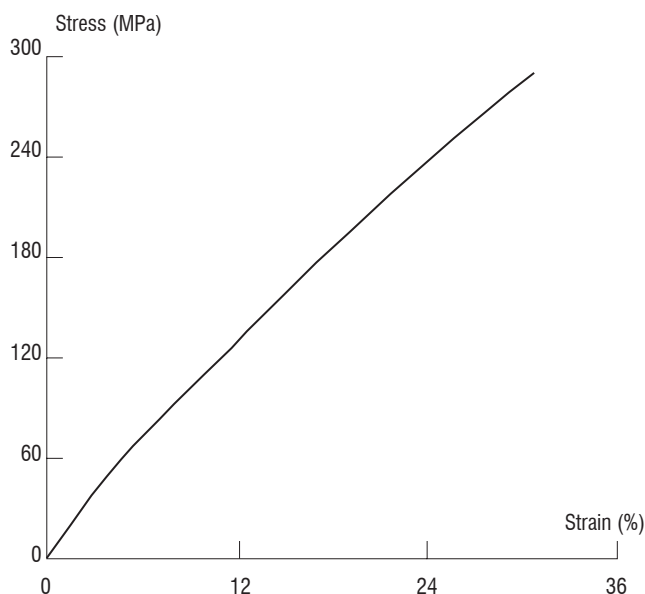


Figure 8 – Tensile stress-strain curves for Nextel TM 610/alumina ceramic composites at room temperature.

## Conclusion

To develop CMCs with a low manufacturing cost and better durability in air at high temperatures compared to SiC/SiC composites with carbon interphase between fiber and matrix, oxide/oxide composites based on weak matrix concept without interphase are under investigation at Onera. Oxide Nextel fibers produced by 3M Company (USA) were selected to reinforce a porous alumina matrix. Infiltration technique was used to infiltrate a submicron alumina powder in 2D satin woven fabrics of Nextel 720. The selected alumina powder is able to sinter at a moderate temperature ( $\leq 1200^\circ\text{C}$ ) with limited shrinkage to avoid matrix multicracking. After optimization of the infiltration and sintering conditions leading to a matrix porosity of 25% and a fiber volume fraction of 40%, a flexural strength of 225 MPa is achieved at  $1150^\circ\text{C}$ . To avoid reductions in mechanical properties after ageing, additional infiltration of zirconium alkoxide in the porosity was assessed and validated. Indeed, this additive limits the matrix sintering and increases its mechanical strength. In parallel, TBCs were studied to improve lifetime and working temperature. From a thermal simulation point of view, the most efficient TBC is an alumina coating with a porosity of 70% (RBAO). Only one millimeter is necessary to keep the surface of the composite at  $1100^\circ\text{C}$  in conditions simulating a combustion chamber with gas at  $1500^\circ\text{C}$ . However, debonding of the RBAO TBC from the composite is observed after ageing at  $1200^\circ\text{C}$ . This behavior has been correlated to the difference in CTEs leading to thermal stresses higher than the flexural strength of such an RBAO TBC, which is quite low. On the other hand, a 2 mm thick sintered mullite TBC with porosity of 40% is as efficient as an RBAO TBC and no debonding is observed. To improve the fiber volume fraction up to 50%, composite has been manufactured by using vacuum molding of prepregs layers. Using 2D satin woven fabrics of Nextel 610, higher mechanical performances were obtained and are close to those of SiC/SiC composites manufactured by CVI. This investigation has thus shown that oxide/oxide composites have attained sufficient maturity to develop industrial demonstrators for gas turbine components, such as exhaust parts or combustor chambers ■

## Acknowledgements

The authors would like to thank Dr. R. Valle for valuable discussions.

## References

- [1] M. VAN ROODE, A. SWEDA, K. MORE, J. SUN - *25.000 hour Hybrid Oxide CMC Field Test Summary*. Proceedings of ASME Turbo Expo 2008 : Power for Land, sea and air GT 2008, June 9-13, Berlin, GT 2008-51379, 2008.
- [2] O. SUDRE, A. RAZELL, L. MOLLIEUX, M. HOLMQUIST - *Alumina Single-Crystal Reinforced Alumina Matrix for Combustor Tiles*. 22nd Annual Cocoa Beach Conference and Exposition on Advanced Ceramics, Materials and Structures, Cocoa Beach (FL), January, pp. 20-24, 1998.
- [3] M. PARLIER, M.-H. RITTI - *State of Art and Perspectives for Oxide/Oxide Composites*. Aerospace Science and Technology, Vol. 7, pp. 211-221, 2003.
- [4] M.-Y. HE, J.-W. HUTCHINSON - *Kinking of a Crack out of an Interface*. J. Appl. Mech., Vol. 56, pp. 279-8, 1989.
- [5] D. KOCH, K. TUSHTEV, G. GRATHWOHL - *Ceramic Fiber Composites: Experimental Analysis and Modeling of Mechanical Properties*. Composites Science and Technology, Vol. 68, pp.1165-1172, 2008.
- [6] L.-P. ZAWADA, S.-G. STEEL, S. MALL - *Fatigue Behavior of a Nextel 720 / Alumina (N720/A) Composite at Room and Elevated Temperature*. Ceram. Eng. Sci. Proc., Vol. 22, [3], pp. 695-702, 2001.
- [7] M. WEY - *Utilisation de polymères inorganiques oxydes dans l'élaboration de composites à architecture 3D*. Doctoral Thesis, University of Paris 7, 3rd of December, 1993.
- [8] H. FUJITA, C.-G. LEVI, F.-W. ZOK - *Controlling Mechanical Properties of Porous Mullite /Alumina Mixtures via Precursor-Derived Alumina*. J. Am. Ceram. Soc., Vol. 88, n° 2, pp. 367-375, 2005.
- [9] W.-D. BRENTNALL, M. VAN ROODE, P.-F. NORTON, S. GATES, J.-R. PRICE, O. JIMENEZ, N. MIRIYALA - *Ceramic Gas Turbine Development at Solar Turbines Incorporated*. Progress in ceramic gas turbine development, Vol. 1, chap. 2, pp.155-192, 2002.
- [10] D.-A. STEWART, D.-B. LEISER - *Characterization of the Thermal Conductivity for Fibrous Refractory Insulations*. Proceedings of the 9th Annual Conference on Composites and Advanced Ceramic Engineering and Science Proceedings, Vol. 6, issue 7/8, pp. 769-792, 1985.
- [11] N. CLAUSSEN - *Processing, Reaction Mechanisms and Properties of Oxidation Formed Al<sub>2</sub>O<sub>3</sub> Matrix Composites*. Journal de Physique IV-C7 (3), pp. 1327-1334, 1993.
- [12] S. BERTRAND, T. MICHALET, A. GIRAUD, M. PARLIER, A. BATAILLE, R. DUCLOS, J. CRAMPON - *Processing, Microstructure and Mechanical Strength of Al<sub>2</sub>O<sub>3</sub> Ceramics Reaction Bonded*. Ceramics International , Vol. 29, pp. 735-744, 2003.
- [13] T. MICHALET, M. PARLIER, F. BECLIN, R. DUCLOS, J. CRAMPON - *Elaboration of Low Shrinkage Mullite by Active Filler Controlled Pyrolysis of Siloxanes*. J. Eur. Ceram. Soc., Vol. 22, pp. 143-152, 2002.
- [14] D. DEMANGE, A. BOUVET - *Experimental and Software Tools to Forecast Radiative and Conductive Thermal Transfer in Partially Transparent Material Deposited on Rotating Blades for Turbine Engine*. Aerospace Science and Technology - AST, Vol. 8, n° 4, pp. 321-331, 2004.
- [15] S. TIMOSHENKO - *Analysis of Bimetal Thermostats*. J. Opt. Soc. Amer., Vol. 11, pp. 233-255, 1925.
- [16] R. VALLE, D. LÉVÊQUE, M. PARLIER - *Optimizing Substrate and Intermediate Layers Geometry to Reduce Internal Stresses and Prevent Surface Crack Formation in 2D Multilayered Ceramic Coatings*. J. Eur. Ceram. Soc., Vol. 28, pp. 711-716, 2008.
- [17] M.-B. RUGGLES-WRENN, S.-S. MUSIL, S. MALL, K.-A. KELLER - *Creep Behavior of Nextel 610/Monazite/Alumina Composite at Elevated Temperatures*. Comp. Sci. Techn., Vol. 66, pp. 2089-2099, 2006.
- [18] K. -A. KELLER, TAI-IL MAH, T.-A. PARTHASARATHY, C.-M. COOKE - *Fugitive Interfacial Carbon Coatings for Oxide/Oxide Composites*. J. Amer. Ceram. Soc., Vol. 83, pp. 329-336, 2004.
- [19] D.-B. MARSHALL, J.-B. DAVIS - *Ceramics for Future Power Generation Technology: Fiber Reinforced Oxide Composites*. Current Opinion in solid State and Materials Science. Vol. 5, pp. 283-289, 2001.
- [20] C.-G. LEVI, J.-Y. YANG, B.-J. DALGEISH, F.-W. ZOK, A.-G. EVANS - *Processing and Performance of an All-Oxide Ceramic Composite*. J. Amer. Ceram. Soc., Vol. 81, pp. 2077-2086, 1998.
- [21] C.-G. PAPAKONSTANTINOOU, P. BALAGURU, R.-E. LYON - *Comparative Study of High Temperature Composites*. Composites: part B, Vol. 32, pp. 637-649, 2001.

## Acronyms

CMCs	(Ceramic Matrix Composites)
WICs	(Weak Interface Composites)
NOXICC	(Novel OXIde Ceramic Composites)
TBCs	(Thermal Barrier Coatings)
WMCs	(Weak Matrix Composites)
TEOS	(Tetraethoxysilane)
RBAO	(Reaction Bonded Aluminium Oxide)
RBM	(Reactive Bonded Mullite)
CTE	(Coefficient of Thermal Expansion)
CVI	(Chemical Vapor Infiltration)



**Michel Parlier** Holding an Engineering Diploma from ENSCI (Ecole Nationale Supérieure de Céramiques Industrielles) and having graduated in Materials Science from the University of Paris, he received his Doctorate Degree in Metallurgy (Mechanical Behavior of Materials) from ENSMP (Ecole Nationale Supérieure des Mines de Paris) in 1984. Head of the High Temperature Composite Materials Unit at Onera (Composite Materials and Structures Department), he has been involved in the development of sintering techniques of ceramic powders with specific additives (hot-pressing, reaction bonding, hot isostatic pressing); Chemical Vapor Deposition (CVD) for densification of composites and coatings; Ceramic Matrix Composites (CMC) development (glass-ceramics, oxides and silicon carbide); Oxides derived from Sol-Gel; Silicon carbide derived from organosilicon precursors, low density fibrous thermal insulation; Melt-Growth Composites (MGC) processing routes; thermal, mechanical and microstructural characterizations.



**Marie-Hélène Ritti** is a research engineer working in the Composite Materials and Structures Department (DMSC). After obtaining her Master's degree from the University of Limoges, she joined Onera in 1982. She is mainly involved in the development of Ceramic Matrix composites (CMC) and other oxides materials.



**Aurélie Jankowiak** After graduating from ENSCI in 2005, she received a PhD in Materials Science from the University of Limoges (2008). She has been working since 2009 in the Composite Materials and Structures Department of Onera. Her research field is mainly focused on high temperature materials for functional applications (combustion chambers, engine blades, leading edge).